

Inertial BSN-Based Characterization and Automatic UPDRS Evaluation of the Gait Task of Parkinsonians

Federico Parisi, Gianluigi Ferrari, *Senior Member, IEEE*, Matteo Giuberti, *Member, IEEE*, Laura Contin, Veronica Cimolin, Corrado Azzaro, Giovanni Albani, and Alessandro Mauro

Abstract—The analysis and assessment of motor tasks, such as gait, can provide important information on the progress of neurological disorders such as Parkinson’s disease (PD). In this paper, we design a Body Sensor Network (BSN)-based system for the characterization of gait in Parkinsonians through the extraction of kinematic features, in both time and frequency domains, embedding information on the status of the PD. The gait features extraction is performed on a set of 34 PD patients using a BSN formed by only three inertial nodes (one on the chest and one per thigh). We investigate also the relationship between the selected kinematic features and the Unified Parkinson’s Disease Rating Scale (UPDRS) scores assigned to patients by expert neurologists. This work extends a previously proposed approach to the analysis of leg agility and sit-to-stand tasks and, as such, represents a further step to develop a system for automatic and comprehensive evaluation of different PD motor tasks. A performance analysis of different classification techniques is carried out, showing the feasibility of an automatic (and, eventually, remote) UPDRS scoring system, suitable for tele-health applications in the realm of affective medicine.

Index Terms—Parkinson’s disease (PD), gait analysis, unified Parkinson’s disease rating scale (UPDRS), inertial measurement units (IMU), tele-health

1 INTRODUCTION

POPULATION ageing, in place almost worldwide in recent decades, has led to a growing interest of the scientific community towards neuro-degenerative disorders such as Alzheimer’s and Parkinson’s diseases. In the industrialized countries, the prevalence of PD is about 0.3 percent of the whole population and increases up to 4 percent in people over the age of 80 [1]. Main PD symptoms are related to difficulties in body movements, including bradykinesia, tremor at rest, postural instability, rigidity and gait impairments, beside a general progressive degeneration in the ability of performing motor tasks. All the current therapies for symptoms management, based on the use of dopaminergic drugs, such as Levodopa and dopamine agonist, have shown a loss of

efficacy over time and have also been associated with a variety of side effects including dyskinesias and motor fluctuations, which can even worsen the motor deficiencies induced by the disease. An accurate clinical evaluation of the symptoms’ severity is fundamental to identify an effective therapy but, often, neurologists can rely only on qualitative observations and on their experience.

In order to obtain a more objective assessment of the PD symptoms, semi-quantitative evaluation scales are widely used, such as the Movement Disorder Society—Unified Parkinson’s Disease Rating Scale (MDS-UPDRS) [2], which can help neurologists in determining more accurately the progress degree of the disease. Achieving a high reliability in the evaluation, however, may be difficult and impractical, as it requires a continuous monitoring of the subjects by medical personnel or self-reports by patients (which may likely be unreliable). For this reason, in recent years several works about systems for long-term monitoring of the symptoms [3] and for the automatic evaluation of motor tasks in PD patients, such as the *sit-to-stand* task [4], [5], the *leg agility* task [6], [7], [8], [9], and *tremors* [10], have appeared in the literature.

The assessment of the Gait Task (GT) in Parkinsonians is a widely studied field [11], [12], [13]. Walking, in fact, is the motor task that mostly affects PD patients’ daily life and independence, being representative of the global ability of patients to perform complex movements and also very sensitive to fluctuations between the periods in which the drug’s effect is active and those in which it is not (ON-OFF state fluctuations). Classical Gait Analysis (GA) systems are based on foot switches [14], Ground Reaction Forces (GRFs) [12], and optoelectronic systems [15]. These technologies need to be

- F. Parisi and G. Ferrari are with the CNIT Research Unit of Parma and the Department of Information Engineering, University of Parma, I-43124, Parma, Italy. E-mail: federico.parisi@studenti.unipr.it, gianluigi.ferrari@unipr.it.
- M. Giuberti is with Xsens Technologies B.V., 7500 AN Enschede, The Netherlands. E-mail: matteo.giuberti@xsens.com.
- L. Contin is with Research & Prototyping, Telecom Italia, Turin, Italy. E-mail: laura.contin@telecomitalia.it.
- V. Cimolin is with the Department of Electronics, Information, and Biengineering, Polytechnic of Milan, Italy. E-mail: veronica.cimolin@polimi.it.
- C. Azzaro and G. Albani are with the Division of Neurology and Neurorehabilitation, Istituto Auxologico Italiano IRCCS, Piancavallo (VB), Italy. E-mail: {c.azzaro, g.albani}@auxologico.it.
- A. Mauro is with the Division of Neurology and Neurorehabilitation, Istituto Auxologico Italiano IRCCS, Piancavallo (VB), Italy and the Department of Neurosciences, University of Turin, Italy. E-mail: mauro@auxologico.it.

Manuscript received 28 Feb. 2015; revised 4 Nov. 2015; accepted 19 Mar. 2016. Date of publication 31 Mar. 2016; date of current version 12 Sept. 2016. Recommended for acceptance by G. Fortino and G.Z. Yang. For information on obtaining reprints of this article, please send e-mail to: reprints@ieee.org, and reference the Digital Object Identifier below. Digital Object Identifier no. 10.1109/TAFFC.2016.2549533

used in controlled clinical environments, may be expensive, and often require experienced and specifically trained personnel. Inertial Measurement Unit (IMU)-based GA is currently the most adopted alternative approach, because it is cost-effective, reliable, and easy-to-use [16], [17], [18].

The adoption of this inexpensive and non-intrusive technology to monitor and assess Parkinsonians' symptoms represents an important step in the direction of practical and effective home health care systems, which may connect patients and clinicians, bringing benefits to both of them. In particular, patients, at their homes, would feel more comfortable, relaxed, and motivated to do their exercises. Moreover, they could save time and money, avoiding to go to the ambulatory for each visit. Clinicians, on the other end, would assist a larger number of subjects, who, otherwise, could not be followed continuously by a movement disorder specialist. This would allow doctors to rely on more accurate and up-to-date clinical pictures of the patients [19].

The aim of this work is to accurately characterize gait in Parkinsonians, extracting relevant kinematic features through an IMU-based BSN. In particular, we consider a BSN formed by only three nodes (one on the chest and one per thigh): this makes the proposed system easy-to-use and attractive for affective medicine. We then investigate the relationship between the extracted features and the UPDRS scores assigned by neurologists. Finally, we design a classification system for the automatic assessment of the UPDRS score in the GT.

The preliminary results presented in [20] are extended considering a larger set of patients, new gait parameters (in both time and frequency domains), an improved algorithm for gait cycle segmentation, and, finally, evaluating the performance of an automatic UPDRS score estimation system.

1.1 The Gait Task

MDS-UPDRS is the most popular rating system used in the clinical study of PD and its accuracy and reliability have been proved in different studies [21]. MDS guidelines for the assessment of the motor symptoms, through 18 specific and simple functional tasks, are described in the UPDRS document—Part III [22]. In the following, we focus our attention on the GT.

1.1.1 Task Description

The MDS defines the GT as follows: the patient is asked to walk, at his/her preferred speed, away from the examiner for at least 10 m and in straight line, then to turn around and return to the starting point. This exercise should be performed in an obstacle-free environment and the initial/final acceleration phases should be discarded to avoid border effects in the analysis. The parameters of interest are those strictly related to the gait characteristics, such as: the stride/step amplitude and speed; the cadence; the gait cycle time; parameters related to the turning phase; the variability between left and right steps; and the arm swing. Freezing of gait should be evaluated separately and is not considered in this work. Arm swing will not be considered as well, as no inertial sensor is placed on the arms. This is an interesting extension of our approach.

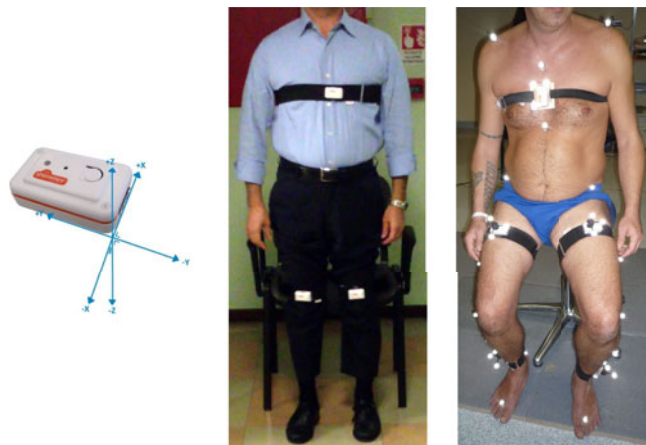


Fig. 1. (a) A Shimmer device (IMU) and its reference coordinate system. The considered experimental testbed in: (b) the actual acquisitions in clinical environment; (c) the optoelectronic validation.

1.1.2 UPDRS Evaluation

By observing the gait characteristics (outlined in Section 1.1.1) during a patient's walk, doctors should assign him/her an integer score between 0 and 4. In particular: a UPDRS score equal to 0 corresponds to normal walking; UPDRS scores 1 and 2 are assigned to patients who can walk independently but present some minor (UPDRS score 1) or substantial (UPDRS score 2) impairments, such as slow walking, short steps, and festination; finally, if the subject cannot walk without any help, it is necessary to evaluate the level of assistance needed to perform the walking task or if he/she cannot walk at all (UPDRS score from 3 to 4). The evaluation of the GT is usually performed without the support of any technological instrument so that the neurologist assesses the task in a qualitative way and relies especially on his/her experience and training. Therefore, assessments may vary from neurologist to neurologist (inter-rater variability) or from one evaluation session to another by the same neurologist (intra-rater variability) [23].

1.2 Paper Structure

The structure of this paper is the following. In Section 2, the experimental set-up, with the details of the used hardware, the set of considered subjects, and the trials' acquisition procedures, is described. In Section 3, we present the methods for the estimation of the parameters which characterize gait, in both time and frequency domains. The obtained experimental results are shown and discussed in Section 4. Conclusions are finally drawn in Section 5.

2 EXPERIMENTAL SET-UP

2.1 Hardware Description

The BSN is formed by Shimmer (Sensing Health with Intelligence, Modularity, Mobility, and Experimental Reusability) nodes [24], i.e., small and low-power wireless sensing platforms that can capture and communicate a wide range of sensed data in real time. A Shimmer node and its reference coordinate system are shown in Fig. 1a. The main module is a compact wearable device (size: 53 mm × 32 mm × 25 mm; weight: 22 g) equipped with: a TI MSP430 microcontroller; Bluetooth (Roving Networks RN-42) and IEEE 802.

15.4-compliant (TI CC2420) radios; an integrated 2 GB microSD card slot; a 450 mAh rechargeable Li-ion battery; and a triaxial accelerometer (Freescale MMA7361). Moreover, the device is designed so that different external sensing modules can be easily connected. The 9DoF Kinematic Sensor expansion module, which is supplied with a triaxial gyroscope (InvenSense 500 series) and a triaxial magnetometer (Honeywell HMC5843), is used. The sampling rate f is set at 102.4 Hz.

For validation purposes, additional data have been recorded for a limited group of subjects, using a Vicon optoelectronic system capable of providing the 3D coordinates of passive markers positioned on specific anatomical landmarks of the subject with an average accuracy of approximately 0.21 mm.

2.2 Subjects and Acquisition Procedure

In this paper, we extend the set of PD patients considered in our preliminary work [20] from 24 to 34. The group of Parkinsonians includes 22 males and 12 females with average age equal to 67.4 years (max = 79 years, min = 31 years) and standard deviation equal to 11.6 years. Furthermore, four healthy subjects (average age equal to 65.5 years and standard deviation equal to 2.88 years), labeled with an UPDRS score equal to 0 in all the trials, have also been included in the set of subjects as a benchmark and to increase the rating range. The number of healthy controls has been limited to four in order to avoid the polarization of the observed results towards the UPDRS 0 class because of the motor performance of non-Parkinsonian (i.e., healthy) subjects.

Each subject is equipped with three Shimmer nodes attached to the body with Velcro straps. The placement of the three sensors (one per thigh, one on the chest) is shown in Fig. 1b. Since this work is part of a more general study, which aims at analyzing multiple UPDRS tasks (namely, the sit-to-stand task [5] and the leg agility task [7], [8], [9], in addition to the GT) with the same BSN, the nodes' configuration has been chosen in order to allow the analysis of the considered tasks without changing the configuration of the nodes, thus: minimizing the patients' stress; simplifying the acquisition procedure; and allowing sequential execution of the tasks. Moreover, the IMUs' placement facilitates the extraction of kinematic parameters through the measurement of angular velocities, inclinations, and accelerations. These measurements are more accurate and reliable than the measurements of positions or displacements, which are derived from the former and usually introduce additional errors in the data analysis. The nodes are oriented trying to align the x axis of their reference system to the upward-downward direction, the y axis to the right-left direction, and the z axis with the antero-posterior direction.

In each trial, the examiner asks the patient to walk, at his/her preferred speed, in an obstacle-free environment for a variable distance between 7 and 15 m and then to turn around and go back to the starting point. The acquisitions have been taken in different locations and, due to the lack of space, it has not always been possible to perform the GT walking continuously for at least 10 m, as the MDS suggests. However, even in the few cases in which the shortest distance (7 m) was travelled, the minimum number of complete gait cycles per leg was between 2 and 4 (after discarding the

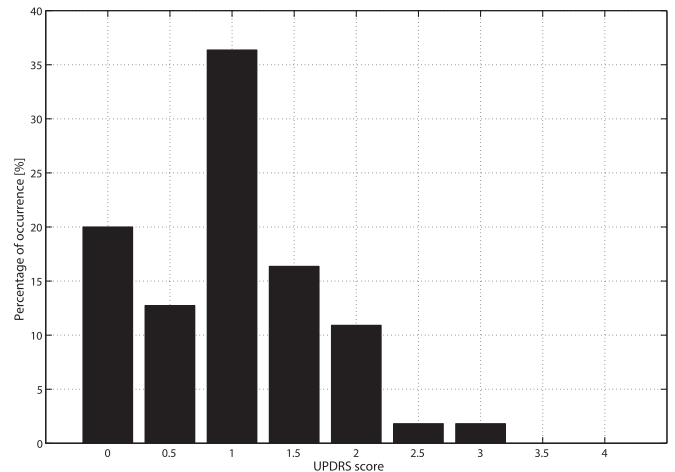


Fig. 2. Distribution of the 55 UPDRS scores assigned to the GT trials.

acceleration and deceleration phases) in both directions, leading to a minimum total number of complete gait cycles per leg between 4 and 8 in the entire trial. The obtained results (presented in the following) show that this minimum number of gait cycles is sufficient to estimate accurately the gait parameters. Moreover, this number is consistent with the number of gait cycles considered in classical GA systems based on other technologies.

A total of 55 complete trials have been acquired, as some patients performed the task in both ON and OFF conditions or at different times. To increase the homogeneity of the assessment, the acquisitions have been evaluated by expert neurologists, using a non-integer scale with intermediate scores (.5) to label the trials in which the neurologists were undecided between consecutive (integer) UPDRS classes. In Fig. 2, the distribution of the 55 UPDRS scores assigned to the GT trials is shown.

The validation of the system was performed by comparing synchronized inertial and optical data on a heterogeneous subgroup of five persons (three males and two females), including both healthy subjects (3) and Parkinsonians (2). The testbed for data validation is shown in Fig. 1c. The details on the optoelectronic-based validation can be found in [9].

3 GAIT CHARACTERIZATION

3.1 Gait Features in the Time Domain

We first analyze gait in the time domain. Besides extracting spatio-temporal parameters and kinematic variables used in classical GA, we consider other features based on the auto-correlation of the accelerometric signal to detect periodic patterns in gait.

3.1.1 Temporal Parameters

Even though the human gait is a complex movement that involves many muscles and joints, it normally has a relevant rhythmic and repetitive component which allows one to segment it into simpler blocks, denoted as *gait cycles*. Two fundamental events per leg are needed to identify a complete gait cycle and all the other temporal parameters which define the different gait phases: the Heel strike (*HS*) (i.e., the instant at which the foot touches the ground) and the Toe-off (*TO*) (i.e., the instant at which the foot leaves the ground). In particular,

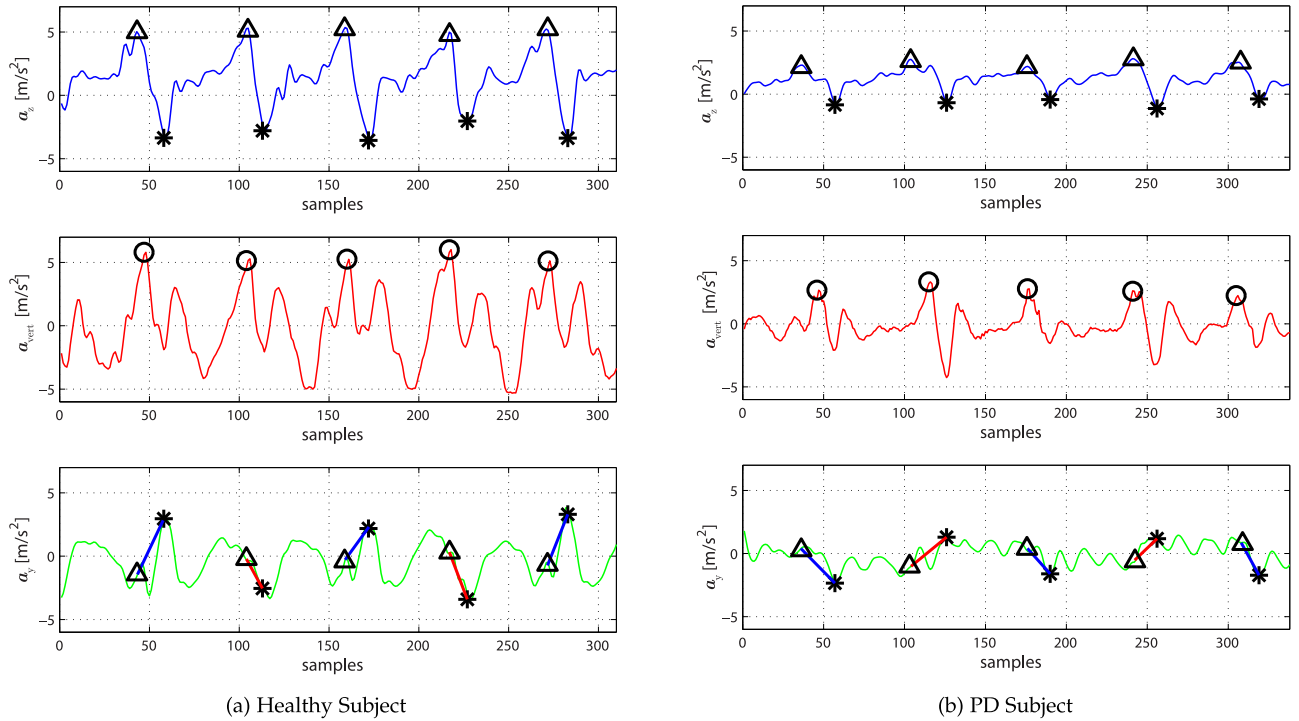


Fig. 3. Recorded trunk accelerations for (a) a healthy subject and (b) a Parkinsonian with mild symptoms (UPDRS score equal to 1.5). Circles represents peaks in the linear vertical acceleration a_{vert} . Triangles and asterisks on the antero-posterior acceleration a_z denote, respectively, HS and TO events. In the medio-lateral acceleration a_y HS points are connected with following TO points by a line whose slope allows to discriminate left leg (blue line, positive slope) from right leg features (red line, negative slope).

a gait cycle starts with the HS of a foot and ends with the following HS of the same foot. The complete sequence of events, considering for example a gait cycle starting with the right leg,¹ is the following: right HS (HS_R), left TO (TO_L), left HS (HS_L), right TO (TO_R), right HS (HS_R).

In order to identify the fundamental events for each gait cycle, we propose a novel approach, based on proper processing of accelerometric signals of the chest-mounted IMU, which improves the accuracy of the algorithm described in [20]. The vertical, the medio-lateral, and the antero-posterior components of the acceleration are denoted as \mathbf{a}_x , \mathbf{a}_y , and \mathbf{a}_z , respectively.

By following a heuristic approach, a preliminary visual investigation was performed detecting manually the HS and TO events and labeling them from the optoelectronic ground truth data synchronized with the accelerometer signal. We observed that HS events are usually located in proximity of negative and positive peaks in vertical and frontal accelerations, respectively. Physically, this is due to the fact that, just before the HS instant, the trunk reaches the maximum vertical acceleration intensity (with negative sign because the body is falling toward the ground) and also the maximum frontal acceleration (because the body is moving forward and then suddenly decelerates after the foot contact). In our previous work [20], the negative peaks in vertical acceleration were chosen to estimate the HS instants because the acceleration in the upward-downward direction is usually sharper and stronger than the one in the antero-posterior direction and maintains a more uniform pattern among different walking styles or increasing gait

impairments. In the current work, the algorithm for the identification of the HS instants is refined to achieve a better accuracy, taking into account both the acceleration components. In particular, the peaks in a preprocessed version of the vertical acceleration have been used to define a limited region in which peaks in frontal acceleration, corresponding to the HS events, are searched. The estimation of the TO instants and the automatic labeling of the right/left events are performed according to the approach described in [20], considering the local minima after the HS s in the antero-posterior acceleration and the projection of HS s' and TO s' instants in the medio-lateral acceleration, respectively (the details of this procedure are given in the following).

Typical acceleration patterns of a healthy subject and of a Parkinsonian, measured by the accelerometer placed on the trunk for a few consecutive gait cycles, are shown in Fig. 3, where the sampling interval, denoted as Δ , is equal to $\frac{1}{f} = 9.76$ ms. Although the accelerations, in a normally walking (healthy) person, are more defined and have wider excursions, the described features can be easily identified also in the accelerometric data recorded for a Parkinsonian.

The algorithm used for the estimation of the HS and TO events can be detailed as follows. First of all, the raw accelerometric signals are low-pass filtered with a fourth-order zero-lag Butterworth filter with bandwidth equal to 20 Hz: this is expedient to reduce high frequency noise components. In order to avoid attenuation effects in the vertical acceleration \mathbf{a}_x , caused by an imperfect alignment of the sensors with the direction of the gravity, the three-dimensional orientation of the Shimmer node, in the Earth's frame (i.e., the reference system in which the x axis points toward the magnetic north, the y axis points toward east, and the z axis points

1. If not specified, we always refer to a right gait cycle.

downward, toward the center of the Earth, according to the direction of the gravity), is estimated through an orientation filter based on a gradient descent algorithm [25]. The contribution of the gravity (9.81 m/s^2 in the z axis) is then subtracted from the acceleration component in the Earth frame's z axis: the effective linear vertical acceleration, denoted as \mathbf{a}_{vert} , is thus obtained. We remark that, since \mathbf{a}_{vert} refers to the Earth frame, downward accelerations are positive, whereas upward accelerations are negative. For this reason, as shown in the second row of Fig. 3, while the body is falling towards the ground (i.e., just before an HS event) the values of \mathbf{a}_{vert} are positive and their peaks are good candidates to accurately estimate a step/stride. Therefore, we now describe the approach followed to estimate the instants corresponding to the peaks.

In order to make the peak selection more accurate, the signal \mathbf{a}_{vert} is further processed as follows. First of all, \mathbf{a}_{vert} is low-pass filtered (using a fourth-order zero-lag Butterworth filter with cut-off frequency set to 5 Hz) to make it smoother. Then, the filtered signal is shifted by adding a quantity equal to the minimum value (with sign) of \mathbf{a}_{vert} measured in the entire trial, in order to have only positive values. Finally, since we observed that the highest peaks were always higher than 1 m/s^2 , the obtained signal is squared to magnify further highest peaks. At this point, the resulting signal, denoted as $\mathbf{a}_{\text{preproc}}$, is analyzed to extract instants of the highest positive peaks, generally denoted as $\mathbf{peak}_{\text{vert}} = \{peak_{\text{vert}}(j)\}_{j=1}^{N_{\text{peaks}}}$, where N_{peaks} is the number of highest peaks in the trial, which approximately identify the HS instants. In particular, in order to detect only the correct peaks and discard those related to other gait cycle's phases (different from the HS instants), the Matlab function `findpeaks(data, 'MinPeakHeight', Th_{height} , 'MinPeakDistance', Th_{distance})` is used, where: $data$ is the signal in which the peaks should be searched ($\mathbf{a}_{\text{preproc}}$ in this case); ('MinPeakHeight', Th_{height}) and ('MinPeakDistance', Th_{distance}) are (name, value) pair arguments, which impose constraints for refining the peaks' selection procedure. More specifically: the former imposes to consider as possible candidates for peak instants only the positive peaks in $\mathbf{a}_{\text{preproc}}$ with a height greater than a threshold, denoted as Th_{height} (dimension: $[\text{m/s}^2]$), whereas all the others are discarded; the latter imposes that the distances (in terms of samples) between consecutive selected peaks, i.e., $\{peak_{\text{vert}}(j) - peak_{\text{vert}}(j-1)\}_{j=2}^{N_{\text{peaks}}}$, are larger than another threshold, denoted as Th_{distance} (dimension: [s]), to avoid considering, as valid, peaks higher than Th_{height} but pair-wise too close to represent consecutive HS events. The values of these two thresholds have been chosen on the basis of the trunk acceleration patterns observed in both healthy subjects and PD patients. In particular, Th_{height} is set to 25 percent of the maximum value of the signal $\mathbf{a}_{\text{preproc}}$ measured in the considered trial, whereas Th_{distance} is set to 40 samples (approximately 390 ms), assuming that the time intervals between consecutive steps are always longer than 0.39 s for both healthy controls and PD patients.

For each instant $peak_{\text{vert}}(j)$ ($j = 1, \dots, N_{\text{peaks}}$), the peaks in antero-posterior acceleration, coinciding with the actual HS instants, are searched in the interval $(peak_{\text{vert}}(j) - 250 \text{ ms}, peak_{\text{vert}}(j) + 50 \text{ ms})$ and labeled as $\{peak_{HS}(j)\}$. Similarly, local minima in the antero-posterior acceleration are searched

inside the interval $(peak_{HS}(j), peak_{HS}(j) + 250 \text{ ms})$. The nearest one, after $peak_{HS}(j)$, is selected as TO . Finally, to correctly label the features for each leg, we consider the slope m of the line passing through the value of the medio-lateral acceleration sample, corresponding to the instant of the first detected HS (denoted as HS_1), and the value of the sample coinciding with the following TO instant (denoted as TO_1). If $m \geq 0$, then a left gait cycle is starting, so that HS_1 is labeled as HS_L and the contralateral TO_1 as TO_R ; if $m \leq 0$, HS_1 is labeled as HS_R and TO_1 as TO_L . The following HS and TO are labeled consequently, alternating right and left labels.

The designed algorithm differs from typical trunk-accelerometry approaches for temporal parameters identifications proposed in the literature, such as the one by Zijlstra [17]. In particular, we use a sensor placed on the chest, not on the dorsal side of the trunk, and we consider all the components of the acceleration (including the linear vertical acceleration) to detect the events of interest.

Once all the HS s and TO s have been identified for both legs, the following temporal parameters can be calculated for the k th gait cycle.

- Gait Cycle Time (GCT) (dimension: [s]): the time interval between the HS of a foot to the next HS of the same foot. In particular:

$$GCT_{R/L}(k) = HS_{R/L}(k+1) - HS_{R/L}(k).$$

- Stance Time (ST) (adimensional, % of GCT): the time percentage (relative to the corresponding gait cycle) during which a foot is in contact with the ground. In particular:

$$ST_{R/L}(k) = 100 \times \frac{TO_{R/L}(k) - HS_{R/L}(k)}{GCT_{R/L}(k)}.$$

- Swing Time (SW) (adimensional, % of GCT): the time percentage (relative to the considered gait cycle) during which a foot is not in contact with the ground. In particular:

$$SW_{R/L}(k) = 100 - ST_{R/L}(k).$$

- Double Support (DS) (adimensional, % of GCT): the time percentage (relative to the considered gait cycle) during which both feet are in contact with the ground. This happens twice during a gait cycle: at the beginning and at the end of one foot's stance phase. The first DS phase is denoted as Initial Double Support (IDS) and the second one is denoted as Terminal Double Support (TDS). They can be expressed as follows:

$$IDS(k) = 100 \times \frac{TO_L(k) - HS_R(k)}{GCT(k)}$$

$$TDS(k) = 100 \times \frac{TO_R(k) - HS_L(k)}{GCT(k)}.$$

Finally, the DS can be given the following expression:

$$DS(k) = IDS(k) + TDS(k).$$

A quantity related to DS, denoted as *Limp*, is defined as follows:

$$Limp(k) = |IDS(k) - TDS(k)|.$$

3.1.2 Spatial Parameters

The most commonly considered spatial parameters for gait characterization are the following.

- Stride Length (*SL*) (adimensional: % of subject's height): the distance travelled from the *HS* of one foot to the following *HS* of the same foot (i.e., a stride).
- Stride Velocity (*SV*) (dimension: [% of subject's height/s]): the average linear velocity of a foot during a stride.
- Step Length (*StepL_{R/L}*) (adimensional: % of subject's height): the distance travelled from the *HS* of one foot to the *HS* of the other foot (i.e., a step).
- Step Velocity (*StepV_{R/L}*) (dimension: [% of subject's height/s]): the average linear velocity of a foot during a step.

As for the temporal features, step length and velocity are estimated using only the accelerometer placed on the chest. In the literature, different mathematical models exist for the description of the body movements during walking. One of these models simply considers human gait as an inverted pendulum in which the vertical displacement *h* (dimension: [m]) of the Center of Mass (CoM) can be used to estimate the forward distance *D* (dimension: [m]) traversed at each step. Usually, while a person is walking, the CoM lies within the pelvis but its movements have often been approximated using a sensor device placed in proximity of the second sacral vertebrae [17]. In the same way, in our case we assume that the vertical displacement of the sensor attached to the chest and the one of the CoM are similar. As described in [17], the relationship between vertical and forward displacements is given by the following equation:

$$D = 2K\sqrt{2\ell h - h^2}, \quad (1)$$

where ℓ is the leg length (dimension: [m]) and *K* is an empirically calibrated constant (adimensional). The vertical displacement *h* can be obtained by double integration of the linear vertical acceleration $\mathbf{a}_{\text{vert}} = \{a_{\text{vert}}(i)\}_{i=0}^{N-1}$ (dimension: [m/s²]), where *N* is the length of the signal \mathbf{a}_{vert} . More precisely, the vertical velocity $\mathbf{v}_{\text{vert}} = \{v_{\text{vert}}(i)\}_{i=0}^{N-1}$ (dimension: [m/s]) of the trunk at the *i*th sample can be computed as

$$v_{\text{vert}}(i) = v_{\text{vert}}(i-1) + a_{\text{vert}}(i)\Delta i = 1, \dots, N-1$$

where: $v_{\text{vert}}(0)$ is assumed to be equal to 0; Δ corresponds the sampling period (dimension: [s]); and \cdot . Then, the position $\mathbf{p}_{\text{vert}} = \{p_{\text{vert}}(i)\}_{i=0}^{N-1}$ (dimension: [m]) of the trunk at the *i*th sample can be expressed as

$$p_{\text{vert}}(i) = p_{\text{vert}}(i-1) + v_{\text{vert}}(i)\Delta i = 1, \dots, N-1,$$

where $p_{\text{vert}}(0)$ is set to 0. The position data \mathbf{p}_{vert} are finally high-pass filtered (using a fourth-order zero-lag Butterworth filter with cut-off frequency set to 0.1 Hz), to remove integration drift, and the total displacement amplitude is then calculated as the difference between the maximum and

the minimum values of the trunk position during each step cycle (i.e., the time interval between the *HS* of one foot and the *HS* of the other foot). Considering the *k*th gait cycle, the vertical displacement of the trunk for the right step ($h_R(k)$, dimension: [m]) can be given by the following expression:

$$h_R(k) = \max_{i=HS_R(k)}^{HS_L(k)} p_{\text{vert}}(i) - \min_{i=HS_R(k)}^{HS_L(k)} p_{\text{vert}}(i),$$

where $HS_R(k)$ ($HS_L(k)$) indicates the first sample of the *k*th *HS* for the right (left) leg. The value of the vertical displacement during a left step ($h_L(k)$) can be calculated in the same way. The step lengths (*StepL_{R/L}*) are estimated using (1). The step velocities (*StepV_{R/L}*) are obtained from the step lengths and the duration of the step cycles. Stride spatial parameters can be obtained by adding the values of the features associated with the right and left steps for each gait cycle. Finally, all the values for the spatial parameters, which are initially calculated in meters, are expressed as percentage of the height of the considered subject.²

3.1.3 Additional Features

Thigh's Range of Rotation

Measuring the joint angles and segment inclinations of the lower limbs may provide important information about the characteristics of the movements during gait [26]. The used sensor configuration (including one node per thigh) allows to retrieve only the data regarding the flexion/extension of the thighs.

The angular rate signal measured by the gyroscopes on both legs can be integrated, during each gait cycle, in order to find the instantaneous inclination angle of the thighs' segments. From the thigh angular velocity signal $\omega = \{\omega(i)\}_{i=0}^{N_\omega-1}$ (dimension: [deg/s]), where N_ω is the length of the signal ω , and the sampling period Δ , the value of the angle $\theta = \{\theta(i)\}_{i=0}^{N_\omega-1}$ (dimension: [deg]) can be calculated for the *i*th sample using the following equation:

$$\theta(i) = \theta(i-1) + \omega(i)\Delta i = 1, \dots, N_\omega - 1.$$

The initial angle $\theta(0)$, at the beginning of each cycle, is set to zero. The Range of Rotation (RoR) (dimension: [deg]) of the right thigh (the RoR of the left thigh can be calculated in the same way), inside the *k*th gait cycle, is assumed to be equal to the difference between the maximum and the minimum values of the instantaneous angle, i.e.:

$$\text{Thigh RoR}_R(k) = \max_{i=HS_R(k)}^{HS_R(k+1)} \theta(i) - \min_{i=HS_R(k)}^{HS_R(k+1)} \theta(i).$$

During the experiments, we also collected, in each gait cycle, the maximum value of the angular velocity, denoted as $\text{Max } \omega_{R/L}$, for both thighs.

Autocorrelation-Based Features

As mentioned at the beginning of Section 3.1.1, the movement of the body during walking has a strong repetitive component and the measured acceleration signals reveal

2. Differently from our previous work [20], we use the % of subject's height as measurement unit for the spatial parameters to avoid errors related to different leg lengths.

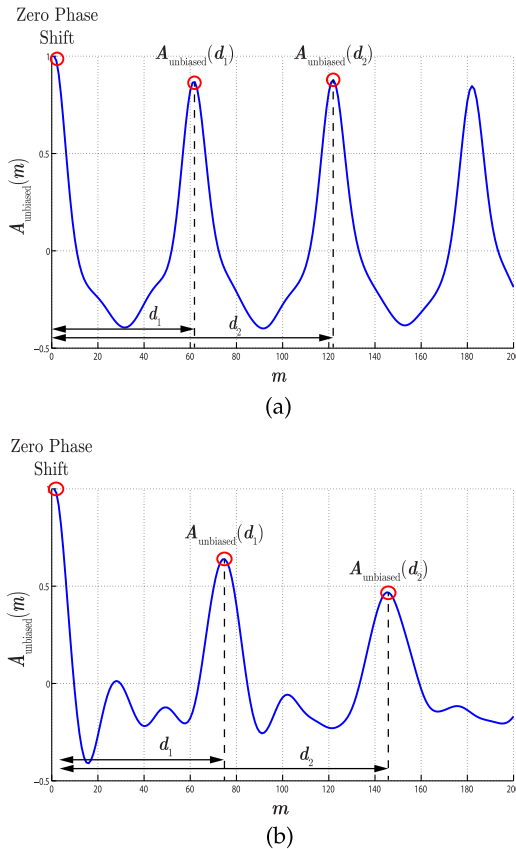


Fig. 4. Unbiased autocorrelation sequences computed from the vertical trunk acceleration for: (a) a healthy subject and (b) a PD patient (UPDRS equal to 2).

periodic patterns which can be estimated computing the autocorrelation of the signal sequence. In [27], the authors show that the autocorrelation of accelerometric signals, recorded with a trunk-mounted sensor, can be used to estimate some relevant gait parameters in a simple way. A brief overview of the details of the algorithm used to calculate these parameters is now presented.

The raw autocorrelation coefficient A of the linear vertical trunk acceleration \mathbf{a}_{vert} , defined as the sum of the products between each sample $a_{\text{vert}}(i)$ ($i = 0, 1, \dots, N-1$) and its time lagged replication $a_{\text{vert}}(i+m)$, is computed as follows:

$$A(m) = \sum_{i=1}^{N-|m|} a_{\text{vert}}(i)a_{\text{vert}}(i+m),$$

where the lag parameter m represents the phase shift (in terms of samples) and may be any positive integer smaller than N . The unbiased³ autocorrelation can be calculated dividing $A(m)$ by the number of samples representing the overlapping part of the time series and the time-lagged replication, i.e.:

$$A_{\text{unbiased}}(m) = \frac{A(m)}{N - |m|}.$$

3. We use the unbiased autocorrelation to avoid the attenuations in amplitudes due to the increasing value of the lag parameter m that occur in the biased version of the autocorrelation.

In Fig. 4, the autocorrelation $A_{\text{unbiased}}(m)$ is shown for both (a) a healthy subject and (b) a PD patient (UPDRS score equal to 2). Only the right half portion of the autocorrelation sequence, properly normalized to 1, has been considered because of its symmetry with respect to the zero phase shift. In both subfigures, one can observe that, besides the maximum at the zero phase shift ($m = 0$), the amplitude of the autocorrelation coefficient presents several peaks for increasing values of m . The first dominant period d_1 is located in correspondence to the first peak after the zero phase shift and represents the phase shift associated with one step. The amplitude of the autocorrelation coefficient in this point, denoted as $A_{\text{unbiased}}(d_1)$, is representative of the regularity of the vertical acceleration signal between steps. This is due to the fact that the amplitude of the autocorrelation at a certain point will be large if the original signal presents regular patterns with a periodicity similar to the phase shift corresponding to the considered point. Similarly, the following peak indicates the second dominant period d_2 , which corresponds to the stride phase shift, and the value of the autocorrelation $A_{\text{unbiased}}(d_2)$ is representative of the stride regularity.

Given the previous defined variables associated with the autocorrelation $A_{\text{unbiased}}(m)$, the following parameters can be defined:

- Cadence (C) (dimension: [steps/minute]): number of steps per minute. In particular:

$$C = \frac{60f}{d_1},$$

where f is the sampling rate (dimension: [sample/s]) at which the accelerometer signal has been recorded (see Section 2.1).

- Regularity (R) (adimensional): representative of the periodicity of the subject's steps/strides. In particular:

$$R_{\text{step}} = A_{\text{unbiased}}(d_1),$$

$$R_{\text{stride}} = A_{\text{unbiased}}(d_2).$$

The closer to 1 $R_{\text{step/stride}}$, the higher the regularity in steps/strides.

- Symmetry (S) (adimensional): ratio between step and stride regularities. In particular:

$$S = \frac{A_{\text{unbiased}}(d_1)}{A_{\text{unbiased}}(d_2)}.$$

Values of S close to 1 indicate a high symmetry between steps and strides.

3.2 Gait Features in the Frequency Domain

We now investigate the possibility to extract additional information about the gait characteristics of a walking subject by analyzing the collected BSN-based inertial signals in the frequency domain. For simplicity, we take into account only the accelerometric signal of the sensor placed on the chest. In particular, we consider the estimated vertical linear acceleration (\mathbf{a}_{vert}) together with the lateral (\mathbf{a}_y) and antero-posterior (\mathbf{a}_z) components of the trunk acceleration. The signals are preliminary filtered with a fourth-order zero-lag

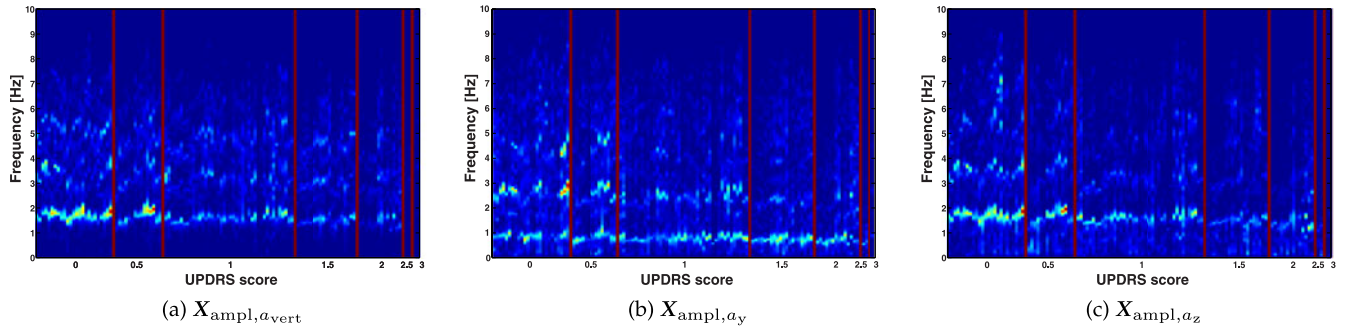


Fig. 5. Two-dimensional representation of the amplitude spectrum of (a) the linear vertical trunk acceleration a_{vert} , (b) the lateral trunk acceleration a_y , and (c) the frontal trunk acceleration a_z , for all available GT trials (one vertical line per trial). The magnitude of the spectrum is mapped to a color that ranges from blue (lowest values) to red (highest values). The GT trials are sorted in ascending order and grouped by UPDRS scores (from 0 to 3), separated by a vertical red line.

Butterworth filter with bandwidth equal to 20 Hz and properly segmented in order to exclude initial and final acceleration/deceleration phases and to avoid the introduction of additional noise. The Discrete Fourier Transforms (DFTs) of the signals are computed using a Fast Fourier Transform (FFT) algorithm for each GT trial. Considering the linear vertical acceleration a_{vert} , the k th component of the spectrum $X_{a_{\text{vert}}} = \{X_{a_{\text{vert}}}(k)\}_{k=0}^{N-1}$ can be computed as follows:

$$X_{a_{\text{vert}}}(k) = \sum_{n=0}^{N-1} a_{\text{vert}}(n) e^{-jk\frac{2\pi}{N}n} \quad k = 0, \dots, N-1.$$

The corresponding amplitude spectrum, denoted as $X_{\text{ampl},a_{\text{vert}}}$, is obtained by dividing the absolute value of $X_{a_{\text{vert}}}$ by N :

$$X_{\text{ampl},a_{\text{vert}}} = \frac{|X_{a_{\text{vert}}}|}{N}.$$

In the same way, the spectra of the lateral ($X_{a_y} = \{X_{a_y}(k)\}_{k=0}^{N-1}$) and the antero-posterior ($X_{a_z} = \{X_{a_z}(k)\}_{k=0}^{N-1}$) accelerations can be computed.

In Fig. 5, the amplitude spectra $X_{\text{ampl},a_{\text{vert}}}$, X_{ampl,a_y} , and X_{ampl,a_z} , associated with all the 55 GT trials, are shown. The spectra have been grouped according to the UPDRS score assigned to the trials by neurologists and sorted in ascending order (from UPDRS 0 to 3). It can be observed that spectrum amplitude peaks are centered in correspondence to step frequency (approximately around 2 Hz) and their magnitudes tend to decrease moving from low to high UPDRS values (from left to right): the higher the UPDRS, the “less powerful” the movement. This intuitive consideration can be translated into a new feature representative of the “power” of the movement. For the signal a_{vert} , we define the spectrum power $P_{a_{\text{vert}}}$ as follows:

$$P_{a_{\text{vert}}} \triangleq \frac{1}{N} \sum_{k=0}^{N-1} (X_{a_{\text{vert}}}(k))^2.$$

Similarly, the spectrum powers of X_{a_y} , denoted as P_{a_y} , and of X_{a_z} , denoted as P_{a_z} , are computed. Finally, the feature P_{sum} , which takes into account the power of all the components, is computed as follows:

$$P_{\text{sum}} = P_{a_{\text{vert}}} + P_{a_y} + P_{a_z}.$$

3.3 Overall Features

For ease of readability, in Table 1 we summarize all the 29 considered features.⁴

4 RESULTS AND DISCUSSION

4.1 System Validation

A preliminary validation procedure was performed in order to verify the consistency between features’ estimation through the inertial BSN and through the optoelectronic reference system. The estimation errors, defined as the difference between the values obtained using our inertial measurement system and the ground truth (given by the optoelectronic system), considering various spatio-temporal parameters, are shown in Table 2. The average errors are comparable to those obtained in other studies, with both similar and different methods [16], [17], [28], and are sufficiently low to be considered almost negligible for our purposes. In particular, the errors in the detection of *HS* and *TO* events are likely to be systematic (they have always the same sign) and could thus be corrected at a later stage. For what concerns the measure of the thighs’ inclination, the system validation has already been performed in [9] with similar precision.

4.2 Features Analysis

As anticipated in Section 1, the aim of this work is to investigate the connection between gait features in PD patients and the UPDRS scores assigned to them by clinicians. Our ultimate goal is to define a protocol for automatic UPDRS scoring of Parkinsonians.

In Fig. 6, the average values of all 29 considered features, calculated over all the GT trials belonging to each UPDRS class are shown. The features’ values have been normalized between 0 and 1, matching the maximum value of each feature to 1. It can be observed that some of the displayed parameters reveal clear monotonic trends as functions of the UPDRS score. For ease of visualization, in the following we consider only a subset of the 29 features, trying to maintain the relevant information about the gait characteristics and to reduce redundancy. The parameters with right and left components have been replaced with the arithmetic average of the two values. For instance, the new feature GCT_{mean} is computed by

4. For some features, only the formula associated with the right leg is shown for lack of space. The formula for the left leg is straight forward.

TABLE 1
Summary of All the 29 Considered Gait Features

Feature	Dimension	Formula
Temporal Features		
<i>Gait Cycle Time</i> : the time interval between the <i>HS</i> of a foot to the next <i>HS</i> of the same foot.	s	$GCT_{R/L}(k) = HS_{R/L}(k+1) - HS_{R/L}(k)$
<i>Stance Time</i> : portion of the GCT during which a foot is in contact with the ground.	%	$ST_{R/L}(k) = 100 \times \frac{TO_{R/L}(k) - HS_{R/L}(k)}{GCT_{R/L}(k)}$
<i>Swing Time</i> : portion of the GCT during which a foot is not in contact with the ground.	%	$SW_{R/L}(k) = 100 - ST_{R/L}(k)$
<i>Initial Double Support</i> : portion of the GCT during which both feet are in contact with the ground (in the first step of the gait cycle).	%	$IDS(k) = 100 \times \frac{TO_L(k) - HS_R(k)}{GCT(k)}$
<i>Terminal Double Support</i> : portion of the GCT during which both feet are in contact with the ground (in the second step of the gait cycle).	%	$TDS(k) = 100 \times \frac{TO_R(k) - HS_L(k)}{GCT(k)}$
<i>Double Support</i> : total portion of the GCT during which both feet are in contact with the ground.	%	$DS(k) = IDS(k) + TDS(k)$
<i>Limp</i> : difference between IDS and TDS in the same gait cycle (absolute value).	%	$Limp(k) = IDS(k) - TDS(k) $
Spatial Features		
<i>Stride Length</i> : distance travelled during a complete gait cycle.	% of subject's height	$SL(k) = StepL_R(k) + StepL_L(k)$
<i>Stride Velocity</i> : the average linear velocity of a foot during a gait cycle.	% of subject's height/s	$SV(k) = \frac{SL(k)}{GCT(k)}$
<i>Step Length</i> : distance travelled from the <i>HS</i> of one foot to the <i>HS</i> of the contralateral foot (step cycle).	% of subject's height	$StepL_{R/L}(k) = K2\sqrt{2\ell h_{R/L}(k) - h_{R/L}(k)^2}$
<i>Step Velocity</i> : the average linear velocity of a foot during a step cycle	% of subject's height/s	$StepV_R(k) = \frac{StepL_R}{HS_L(k) - HS_R(k)}$
Additional Features		
<i>Thigh Range of Rotation</i> : maximum flexion/extension excursion of the thighs.	deg	$Thigh\ RoR_R(k) = \max_{i \in GCT_R(k)} \theta(i) - \min_{i \in GCT_R(k)} \theta(i)$
<i>Maximum Angular Velocity</i> : maximum value of a thigh's angular velocity in a gait cycle.	deg/s	$\text{Max } \omega_R(k) = \max_{i \in GCT_R(k)} \omega(i)$
<i>Cadence</i> : step number per minute.	steps/minute	$C = \frac{60f}{d_1}$
<i>Step Regularity</i> : measure representative of step periodicity.	adimensional	$R_{\text{step}} = A_{\text{unbiased}}(d_1)$
<i>Stride Regularity</i> : measure representative of stride periodicity.	adimensional	$R_{\text{stride}} = A_{\text{unbiased}}(d_2)$
<i>Symmetry</i> : ratio between step and stride regularity.	adimensional	$S = \frac{A_{\text{unbiased}}(d_1)}{A_{\text{unbiased}}(d_2)}$
Features in the Frequency Domain		
Spectrum Power for the linear vertical acceleration.	adimensional	$P_{\text{avert}} = \frac{1}{N} \sum_{k=0}^{N-1} (X_{\text{avert}}(k))^2$
Spectrum Power for the medio-lateral acceleration.	adimensional	$P_{\text{ay}} = \frac{1}{N} \sum_{k=0}^{N-1} (X_{\text{ay}}(k))^2$
Spectrum Power for the antero-posterior acceleration.	adimensional	$P_{\text{az}} = \frac{1}{N} \sum_{k=0}^{N-1} (X_{\text{az}}(k))^2$
<i>Total Spectrum Power</i> .	adimensional	$P_{\text{sum}} = P_{\text{avert}} + P_{\text{ay}} + P_{\text{az}}$

averaging GCT_R and GCT_L . The 11 features in the reduced set are $\{GCT_{\text{mean}}, ST_{\text{mean}}, DS, Limp, SL, StepV_{\text{mean}}, C, R_{\text{step}}, S, Thigh\ RoR_{\text{mean}}, P_{\text{sum}}\}$. In Fig. 7, the average values of the features in the reduced set, averaged, over all trials, for each UPDRS class, are shown through a radar plot. It can be observed that the values of the temporal parameters, such as GCT , ST , and DS , are generally increasing for increasing UPDRS score, as observed in other works [11]. Patients with gait impairments, in fact, tend to walk more slowly than healthy subjects (walking normally) and remain longer in the double support phase. This, in turn, implies also lower values of cadence C , due to longer GCT s which influence the

number of steps which patients can perform in a minute. It is possible to remark that subjects who present *festinating gait*, i.e., an alteration in gait pattern typical of Parkinsonians, characterised by a quickening and shortening of normal strides, perform short steps with a very high cadence, thus leading to low values of temporal parameters even for high UPDRS scores.

Regarding the spatial parameters and the flexion/extension excursion of the thighs, the trend is clearly decreasing for increasing values of the UPDRS score. SL , $StepV$, and $Thigh\ RoR$ have similar trends, with a reduction of approximately 60 percent between the UPDRS class 0 and the UPDRS

TABLE 2
Estimation Errors for Relevant
Spatio-Temporal Parameters

Parameter	Mean	STD
HS	8.22 ms	17.6 ms
TO	6.83 ms	26.33 ms
GCT_R	0 ms	13.81 ms
GCT_L	16.27 ms	28.74 ms
ST_R	-0.03 %	3.46 %
ST_L	-1.62 %	1.23 %
DS	-0.55 %	4.63 %
C	0.7 steps/min	1.8 steps/min
SL	4.23 cm	4.94 cm

classes 2.5 or 3. This result is consistent with clinical observations of Parkinsonian walking, in which patients with increasing gait impairments perform shorter steps, with reduced velocity and reveal, in general, a more limited movement range in lower limbs [29]. In the same way, R_{step} , which is a feature representative of the homogeneity of the rhythmic component of gait, tends to decrease consistently (almost 70 percent) from healthy subjects (normal walking) to subjects with high UPDRS score. The symmetry of walking, expressed by the feature S , maintains, instead, a low variability across all UPDRS values, except for the UPDRS 3 subject: this seems to be more related to the single subject walking characteristics than to the entire scoring cluster.

Finally, the P_{sum} feature, which synthesizes the frequency-domain gait characterization, shows a very high correlation with the UPDRS score, with a clear monotonic decreasing trend and a range excursion of almost 95 percent between the lowest (0) and the highest (3) UPDRS classes. This behaviour is due to the fact that the overall “power” of the subject’s gait decreases consistently in correspondence to: a reduction in amplitude and velocity of strides; a limited regularity in steps’ cadence; and rigidity or, more generally, movement impairments.

We now analyze two illustrative pairs of features, among those just introduced, to highlight the existence of “parametric trajectories” in terms of UPDRS values. In Fig. 8a, all the stride length/power sum pairs $\{(SL_i, P_{sum,i})\}_{i=1}^{55}$ for all

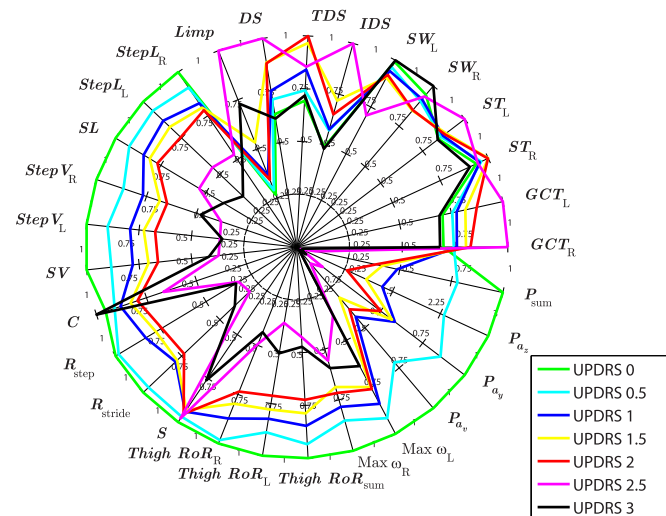


Fig. 6. Average normalized values of all the estimated features for each UPDRS class.

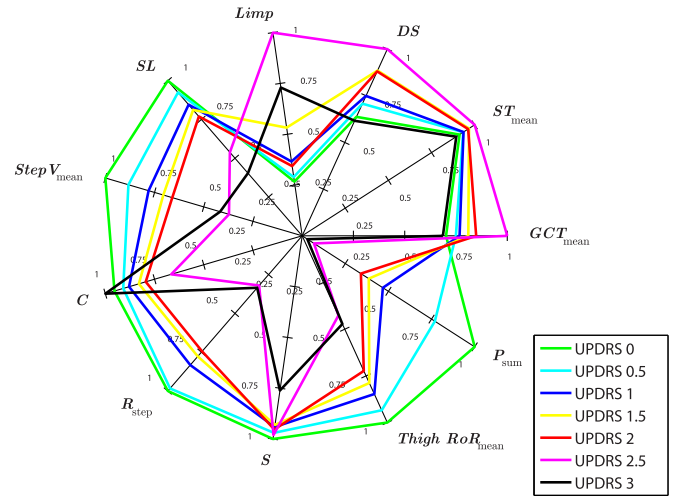


Fig. 7. Average normalized values of the reduced set of features for each UPDRS class.

gait trials are shown on the same two-dimensional plane. Each pair (i.e., a point in the two-dimensional plane) corresponds to a trial and is colored in accordance to the UPDRS score assigned to the patient in the considered test. For each UPDRS score cluster, the centroid is denoted by a star marker (of the same color of its UPDRS class). Furthermore, all centroids are connected by a black piece-wise line, which highlights the parameters’ trend for increasing UPDRS scores. Finally, the (red) exponential fitting and representing a smoothed version of the centroids’ trajectory, is also shown. It can be clearly observed that the centroids move smoothly toward the bottom-left corner for increasing values of the UPDRS score, since both stride length and spectrum total power decrease.

Similarly, in Fig. 8b the pairs $\{(R_{step,i}, Thigh\ RoR_{mean,i})\}_{i=1}^{55}$ are shown on the same two-dimensional plane. The centroids identify a sharp decreasing trajectory toward the bottom-left corner, which corresponds to (i) a more limited rotation range in thighs movements and (ii) a lower step regularity. Note, however, that the pairs of features belonging to UPDRS classes 2.5 and 3 are almost overlapped.

We remark that a few points in both Figs. 8a and 8b are far from the main trajectory because neurologists took into account, for the assignment of the UPDRS scores, other qualitative variables, such as the movement of the upper limbs, which cannot be assessed with the used BSN configuration.

From the obtained results, one can conclude that some gait characteristics, measurable with the proposed inertial BSN, are strongly related to the UPDRS scores assigned to patients by neurologists. Therefore, investigating the feasibility of a classification system for automatic UPDRS score assessment of the GT in Parkinsonians is meaningful.

4.3 Automatic UPDRS Evaluation

For completeness, we have performed a Principal Component Analysis (PCA) on the 11-element reduced set of parameters⁵ introduced above. This allows us to reduce further its dimensionality while retaining most of the variability (i.e., information content) of the original data [30]. For

5. The original 11-dimensional data have been normalized before applying PCA.

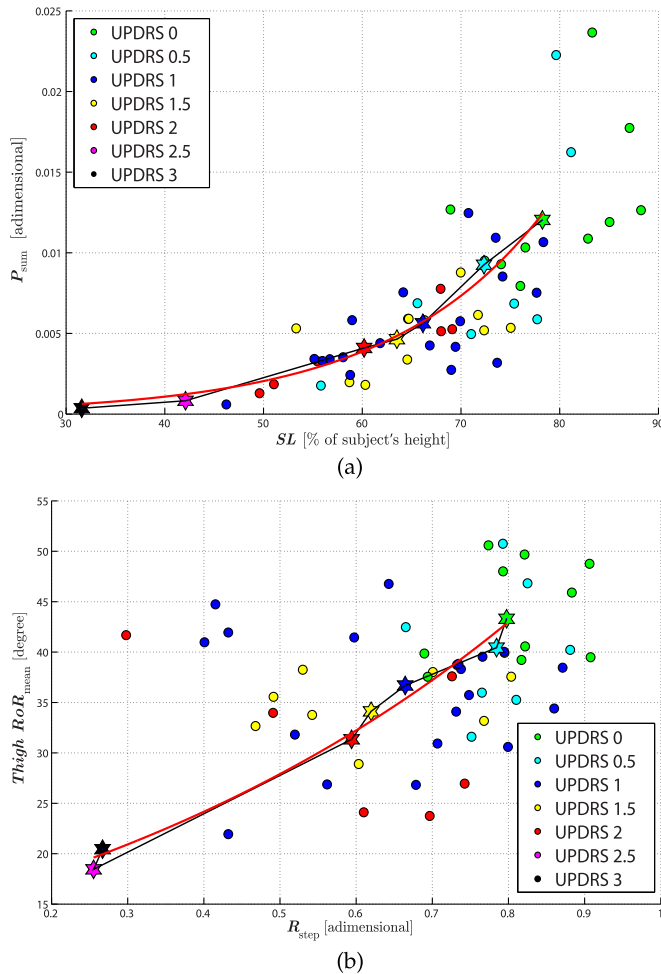


Fig. 8. Average features pairs graphically visualized on the same plane. In (a) the $\{(SL_i, P_{sum,i})\}_{i=1}^{55}$ pairs are considered while in (b) the $\{(R_{step,i}, Thigh\ RoR_{mean,i})\}_{i=1}^{55}$ pairs are displayed. Each point represents a single GT trial and is colored in accordance to its UPDRS score. The centroids of the UPDRS score clusters are shown as colored stars and linked with a black piece-wise line. The red curve is a smoothed (exponential) version of the piece-wise line.

conciseness, no trajectory in the reduced-dimensionality features space is shown.

In order to devise an automatic UPDRS score detection system, we consider three classification methods: Nearest Centroid Classifier (NCC), k Nearest Neighbors (k NN), and Support Vector Machine (SVM) [30]. Several tests have been performed using different system configurations and parameters, both on original data and on PCA-projected data, evaluating the results for: (i) all the combination of the 11 features;⁶ (ii) increasing number of the principal components (from 1 to 11). When the k NN classification method is used, the considered value of k ranges from 0 to 10. A leave-one-out cross-validation method has been adopted to avoid bias in the classification performance. This means that each point of the original dataset is used, in turn, as the new (unknown) point to be classified and the remaining points are used to train the classifiers. The classification procedure returns as

6. We considered the reduced set of features for convenience but experimental results showed that performing the same analysis on the entire set of features does not increase the classification performance.

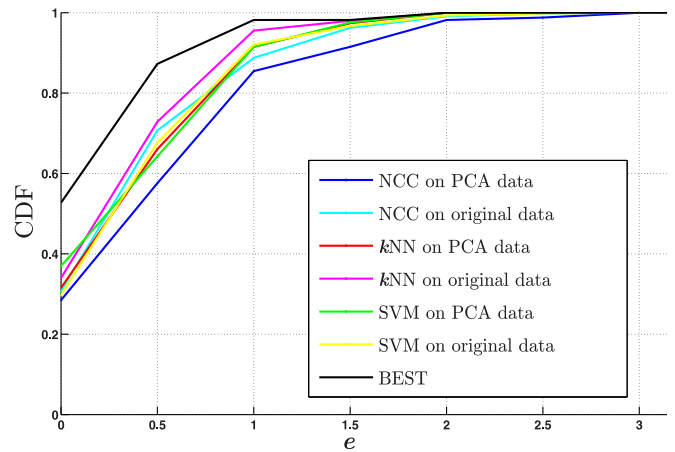


Fig. 9. Average CDFs of the absolute error e evaluated applying NCC, k NN, and SVM on both original and PCA-projected data. The black solid line represents the best CDF, obtained using k NN on the combination of features $(ST_{mean}, StepV_{mean}, S)$ and with $k = 6$.

output an estimated value \hat{u} of the UPDRS score for each sample corresponding to a GT trial.

The absolute UPDRS classification error is defined as follows:

$$e \triangleq |\hat{u} - u|,$$

where u is the actual UPDRS score assigned to trials by a neurologist. To better understand the classification accuracy achieved by the considered algorithms, we compute the Cumulative Distribution Function (CDF) of the error e . In Fig. 9, the average (over all the possible parametric configurations) CDFs obtained by each classifier on both original and PCA-projected data are shown. The Area under the Curve (AuC) is selected as a representative performance metric. It can be observed that, on average, almost all the classification methods achieve similar results. The best accuracy is reached by the k NN algorithm applied on the original dataset, closely followed by SVM and NCC on the same dataset. The use of PCA slightly worsens the classification performance. The CDF which maximizes the AuC, i.e., guarantees the best performance, corresponds to the system using k NN, with $k = 6$, on the subset of features $\{ST_{mean}, StepV_{mean}, S\}$. With this configuration, the system classifies correctly (with $e = 0$) approximately 53 percent of the trials and with $e \leq 1$ almost the entire set of trials (about 98 percent).

Finally, in Fig. 10 we graphically visualize, in a three-dimensional space, the ensemble of realisation of the features triplets $\{ST_{mean,i}, StepV_{mean,i}, S_i\}_{i=1}^{55}$ that achieved the best performance in Fig. 9. Each point corresponds to a trial and centroids are calculated by averaging the features' values among samples belonging to the same UPDRS class. Even though the trajectory identified by the centroids is not as smooth as the trajectories in Fig. 8, a clear trend emerges and allows a good separation between UPDRS classes. This, in turn, corresponds to a robust classification performance.

4.4 Clinical Applications

The performance achieved by the automatic scoring system, discussed in the previous subsection, compares favorably with typical inter/intra-rater variability which can affect neurologists' decisions while assigning UPDRS scores to PD

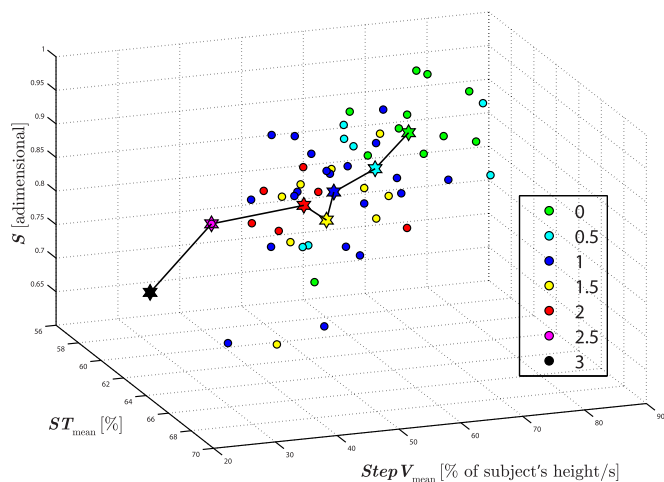


Fig. 10. Three-dimensional representation of the points $\{(ST_{\text{mean},i}, StepV_{\text{mean},i}, S_i)\}_{i=1}^{55}$ associated with the features that achieved the best performance. Each point represents a single GT trial and is colored in accordance to its UPDRS score. The centroids of the UPDRS score clusters are shown as colored stars and linked by a black piece-wise line.

patients [23]. In Fig. 11, the CDF of the error e , defined as the (absolute) difference between the UPDRS scores assigned by the automatic system and the neurologist, is compared with the CDF of the (absolute) difference d between the UPDRS evaluations by two different neurologists. It can be observed that the two CDFs have very similar trends and the maximum variability in the UPDRS scoring between the automatic system and the neurologists is (almost) always within one UPDRS class: this is consistent with the inter-rater variability between clinicians—an exhaustive discussion on this finding, considering different UPDRS tasks (namely, leg agility, sit-to-stand, and gait tasks), is presented in [31]. On the basis of this observation, it can be concluded that the proposed system has the potential to mimic the evaluation performance of medical personnel. Obviously, further investigations on the accuracy and the reliability of the proposed system (using a larger set of patients, a more uniform distribution of scores across all the UPDRS classes, and additional evaluations by more neurologists) should be required to make the performance analysis more meaningful from a statistical point of view.

Nevertheless, the achieved results make the designed system suitable to real applications in the e-health scenario and this, in turn, can provide an added value to the clinical evaluation of the PD. For example, the development of a telemedicine systems for remote monitoring of PD patients could allow the quantitative measurement of motor fluctuations multiple times throughout the day (unlike the usual time-limited evaluation performed in the clinics), providing the neurologists with a more reliable clinical “picture” of the patient and allowing more accurate symptoms’ assessment and management.

5 CONCLUSION

In this paper, an exhaustive characterization of the GT in Parkinsonians, based on the estimation of a large set of gait features, has been performed with the aim of investigating the connection between the measured kinematic variables and the UPDRS scores assigned to patients by neurologists.

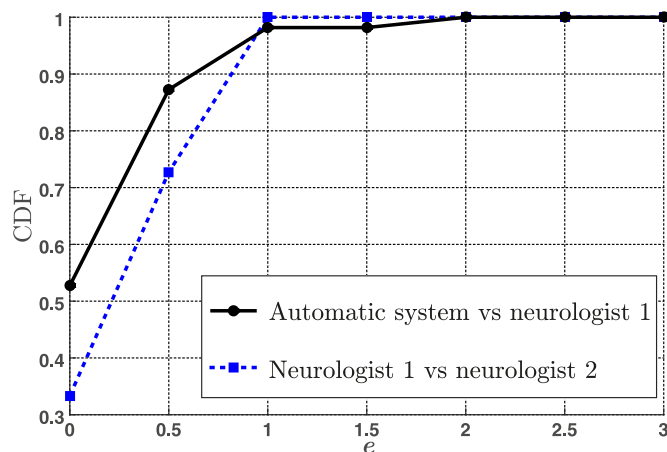


Fig. 11. Comparison between the CDF of the automatic classification error e (i.e., the absolute difference between the (best) score by the automatic system and the score by one of the neurologists) and the absolute difference in the UPDRS scoring between two neurologists.

Different parameters have been calculated using a low-complexity BSN formed by three wearable IMUs. An in-depth analysis of the collected data has been carried out in both time and frequency domains, in order to identify the gait features which are particularly representative of the UPDRS class. In particular, we have focused our attention on (i) a novel approach to estimate temporal parameters from trunk accelerometric signals and (ii) the spectral analysis of the GT, which has revealed a strong connection between the “power” of the movements during walking and the level of gait impairments of the patients. A validation procedure has been carried out to check the accuracy of the proposed system and has been shown that the UPDRS estimation error is almost negligible for the purposes of this work. We have performed an experimental investigation considering 34 PD patients. The observed results show that some parameters, such as SL , $StepV$, R_{step} , $Thigh\ ROR$ and P_{sum} , are clearly related to the UPDRS score and decrease almost linearly with increasing UPDRS values, in accordance with actual clinical observations of walking PD patients. Finally, we have designed and implemented an automatic detection system capable of assessing the GT performed by PD patients and assigning them a suitable UPDRS score. The lowest classification error has been obtained by the k NN algorithm applied on the features $\{ST_{\text{mean}}, StepV_{\text{mean}}, S\}$ and with $k = 6$. The achieved results, together with the possibility to integrate in the same system the automatic evaluation of different UPDRS tasks through the same simple BSN, represent a good starting point for the creation of a tele-health application, easily integrable in an affective computing scenario.

ACKNOWLEDGMENTS

This work is partially supported by the Italian Ministry of Health (RF-2009-1472190).

REFERENCES

- [1] L. M. de Lau and M. Breteler, “Epidemiology of Parkinson’s disease,” *Lancet Neurology*, vol. 5, no. 6, pp. 525–535, Jun. 2006.
- [2] S. Fahn and R. L. Elton, *Recent Developments in Parkinson’s Disease*. Florham Park, NJ, USA: Macmillan Health Care Information, 1987, vol. 2, pp. 153–163.

- [3] B. Chen, S. Patel, T. Buckley, R. Rednic, D. McClure, L. Shih, D. Tarsy, M. Welsh, and P. Bonato, "A web-based system for home monitoring of patients with Parkinson's disease using wearable sensors," *IEEE Trans. Biomed. Eng.*, vol. 58, no. 3, pp. 831–836, Mar. 2011.
- [4] D. Giansanti, G. Maccioni, F. Benvenuti, and V. Macellari, "Inertial measurement units furnish accurate trunk trajectory reconstruction of the sit-to-stand manoeuvre in healthy subjects," *Med. Biol. Eng. Comput.*, vol. 45, no. 10, pp. 969–976, Oct. 2007.
- [5] M. Giuberti, G. Ferrari, L. Contin, V. Cimolin, C. Azzaro, G. Albani, and A. Mauro, "Automatic UPDRS evaluation in the sit-to-stand task of Parkinsonians: Kinematic analysis and comparative outlook on the leg agility task," *IEEE J. Biomed. Health Inform.*, vol. 19, no. 3, pp. 803–814, May 2015.
- [6] D. A. Heldman, D. E. Filipkowski, D. E. Riley, C. M. Whitney, B. L. Walter, S. A. Gunzler, J. P. Giuffrida, and T. O. Mera, "Automated motion sensor quantification of gait and lower extremity bradykinesia," in *Proc. 34th Annu. Int. Conf. IEEE Eng. Med. Biol. Soc.*, Aug. 2012, pp. 1956–1959.
- [7] M. Giuberti, G. Ferrari, L. Contin, V. Cimolin, N. Cau, M. Galli, C. Azzaro, G. Albani, and A. Mauro, "On the characterization of leg agility in patients with Parkinson's disease," in *Proc. 10th Int. Conf. Wearable Implantable Body Sensor Netw.*, May 2013, pp. 1–6.
- [8] M. Giuberti, G. Ferrari, L. Contin, V. Cimolin, C. Azzaro, G. Albani, and A. Mauro, "Linking UPDRS scores and kinematic variables in the leg agility task of Parkinsonians," in *Proc. 11th Int. Conf. Wearable Implantable Body Sensor Netw.*, Jun. 2014, pp. 115–120.
- [9] M. Giuberti, G. Ferrari, L. Contin, V. Cimolin, C. Azzaro, G. Albani, and A. Mauro, "Assigning UPDRS scores in the leg agility task of Parkinsonians: Can it be done through BSN-based kinematic variables?" *IEEE Internet Things J.*, vol. 2, no. 1, pp. 41–51, Mar. 2015.
- [10] A. Salarian, H. Russmann, C. Wider, P. R. Burkhard, F. J. G. Vingerhoets, and K. Aminian, "Quantification of tremor and bradykinesia in Parkinson's disease using a novel ambulatory monitoring system," *IEEE Trans. Biomed. Eng.*, vol. 54, no. 2, pp. 313–322, Feb. 2007.
- [11] A. Salarian, H. Russmann, F. J. G. Vingerhoets, C. Dehollain, Y. Blanc, P. R. Burkhard, and K. Aminian, "Gait assessment in Parkinson's disease: Toward an ambulatory system for long-term monitoring," *IEEE Trans. Biomed. Eng.*, vol. 51, no. 8, pp. 1434–1443, Aug. 2004.
- [12] S. Chien, S. Lin, C. C. Liang, Y. Soong, S. Lin, Y. Hsin, C. Lee, and S. Chen, "The efficacy of quantitative gait analysis by the GAITRite system in evaluation of parkinsonian bradykinesia," *Parkinsonism Related Disorders*, vol. 12, no. 7, pp. 438–442, Oct. 2006.
- [13] S. T. Moore, H. G. MacDougall, J. Gracies, H. S. Cohen, and W. G. Ondo, "Long-term monitoring of gait in Parkinson's disease," *Gait Posture*, vol. 26, no. 2, pp. 200–207, Jul. 2007.
- [14] W. Zijlstra, A. W. Rutgers, and T. W. V. Weerden, "Voluntary and involuntary adaptation of gait in Parkinson's disease," *Gait Posture*, vol. 7, no. 1, pp. 53–63, Jan. 1998.
- [15] A. Ferrari, M. G. Benedetti, E. Pavan, C. Frigo, D. Bettinelli, P. Rabuffetti, P. Crenna, and A. Leardini, "Quantitative comparison of five current protocols in gait analysis," *Gait Posture*, vol. 28, no. 2, pp. 207–216, Aug. 2008.
- [16] K. Aminian, B. Najafi, C. Büla, P. F. Leyvraz, and P. Robert, "Spatio-temporal parameters of gait measured by an ambulatory system using miniature gyroscopes," *J. Biomech.*, vol. 35, no. 5, pp. 689–699, May 2002.
- [17] W. Zijlstra and A. L. Hof, "Assessment of spatio-temporal gait parameters from trunk accelerations during human walking," *Gait Posture*, vol. 18, no. 2, pp. 1–10, Oct. 2003.
- [18] A. Köse, A. Cereatti, and U. Della Croce, "Bilateral step length estimation using a single inertial measurement unit attached to the pelvis," *J. Neuroengin. Rehabil.*, vol. 9, pp. 1–9, Jan. 2012.
- [19] C. Lisetti and C. LeRouge, "Affective computing in tele-home health," in *Proc. 37th Hawaii Int. Conf. Syst. Sciences*, p. 8, Jan. 2004.
- [20] F. Parisi, G. Ferrari, M. Giuberti, L. Contin, V. Cimolin, C. Azzaro, G. Albani, and A. Mauro, "Low-complexity inertial sensor-based characterization of the UPDRS score in the gait task of parkinsonians," in *Proc. 9th Int. Conf. Body Area Netw.*, Sep./Oct. 2014, pp. 69–75.
- [21] A. Siderowf, M. McDermott, K. Kiebertz, K. Blindauer, S. Plumb, and I. Shoulson, "Test-retest reliability of the unified Parkinson's disease rating scale in patients with early Parkinson's disease: Results from a multicenter clinical trial," *Movement Disorder*, vol. 17, no. 4, pp. 758–763, Jul. 2002.
- [22] C. G. Goetz, S. Fahn, P. Martinez-Martin, W. Poewe, C. Sampaio, G. T. Stebbins, M. B. Stern, B. C. Tilley, R. Dodel, B. Dubois, R. Holloway, J. Jankovic, J. Kulisevsky, A. E. Lang, A. Lees, S. Leurgans, P. A. LeWitt, D. Nyenhuis, C. W. Olanow, O. Rascol, A. Schrag, J. A. Teresi, J. J. V. Hilten, and N. LaPelle, "Movement disorder society-sponsored revision of the unified Parkinson's disease rating scale (MDS-UPDRS): Process, format, and clinimetric testing plan," *Movement Disorders*, vol. 22, no. 1, pp. 41–47, Jan. 2007.
- [23] B. Post, M. P. Merkus, R. M. de Bie, R. J. Haan, and J. D. Speelman, "Unified Parkinson's disease rating scale motor examination: are ratings of nurses, residents in neurology, and movement disorders specialists interchangeable?" *Movement Disorders*, vol. 20, no. 12, pp. 1577–1584, Dec. 2005.
- [24] A. Burns, B. R. Greene, M. J. McGrath, T. J. O'Shea, B. Kuris, S. M. Ayer, F. Stroiescu, and V. Cionca, "SHIMMER—A wireless sensor platform for noninvasive biomedical research," *IEEE Sensors J.*, vol. 10, no. 9, pp. 1527–1534, Sep. 2010.
- [25] S. O. H. Madgwick, A. J. L. Harrison, and R. Vaidyanathan, "Estimation of IMU and MARG orientation using a gradient descent algorithm," in *Proc. IEEE Int. Conf. Rehabil. Robot.*, Jun. 2011, pp. 1–7.
- [26] A. Delval, J. Salleron, J. Bourriez, S. Bleuse, C. Moreau, P. Krystkowiak, L. Defebvre, P. Devos, and A. Duhamel, "Kinematic angular parameters in PD: Reliability of joint angle curves and comparison with healthy subjects," *Gait Posture*, vol. 28, no. 3, pp. 495–501, Oct. 2008.
- [27] R. Moe-Nilssen and J. L. Helbostad, "Estimation of gait cycle characteristics by trunk accelerometry," *J. Biomechan.*, vol. 37, no. 1, pp. 121–126, Jan. 2004.
- [28] A. M. Sabatini, C. Martelloni, S. Scapellato, and F. Cavallo, "Assessment of walking features from foot inertial sensing," *IEEE Trans. Biomedical Eng.*, vol. 52, no. 3, pp. 486–494, Mar. 2005.
- [29] G. N. Lewis, W. D. Byblow, and S. E. Walt, "Stride length regulation in Parkinson's disease: The use of extrinsic, visual cues," *Brain*, vol. 123, no. 10, pp. 2077–90, Oct. 2000.
- [30] R. O. Duda, P. E. Hart, and D. G. Stork, *Pattern Classification and Scene Analysis*. 2nd edition. New York, NY, USA: Wiley, 2000.
- [31] F. Parisi, G. Ferrari, M. Giuberti, L. Contin, V. Cimolin, C. Azzaro, G. Albani, and A. Mauro, "Body sensor network-based kinematic characterization and comparative outlook of UPDRS scoring in leg agility, sit-to-stand, and gait tasks in Parkinson's disease," *IEEE J. Biomed. Health Inform.*, vol. 19, no. 6, pp. 1777–1793, Nov. 2015.



Federico Parisi received the BSc and MSc degrees (*summa cum laude*) in computer engineering from the University of Parma, Parma, Italy, in 2010 and 2013, respectively. Since January 2014, he has been the PhD student in information technologies at the Information Engineering Department, University of Parma, Italy, and he is a member of the Wireless Ad-Hoc and Sensor Networks (WASN) Laboratory, supervised by Prof. Gianluigi Ferrari. His research interests include body sensor networks, inertial motion capture and motion reconstruction, gait analysis, mobile applications for e-health and telerehabilitation systems, and pedestrian positioning systems. He was a member of the winning team of the first Body Sensor Networks Hackathon, organized at BSN 2015, Cambridge, MA.



Gianluigi Ferrari (S'96–M'98–SM'12) (<http://www.tlc.unipr.it/ferrari>) is currently an associate professor of Telecommunications with the University of Parma, Parma, Italy. He was a visiting researcher with the University of Southern California, Los Angeles, CA, from 2000 to 2001, Carnegie Mellon University (CMU), Pittsburgh, PA, USA, from 2002 to 2004, King Mongkut's Institute of Technology Ladkrabang (KMILT), Bangkok, Thailand, in 2007, and Université Libre de Bruxelles (ULB), Brussels, Belgium, in 2010. Since 2006, he

has been the coordinator with the Wireless Ad-Hoc and Sensor Networks Laboratory (<http://wasnlab.tlc.unipr.it/>), Department of Information Engineering, University of Parma. He has published extensively in all these fields, collaborating with several private and public institutions. He currently serves on the Editorial Boards of several international journals and is a Springer book series Editor. He received of the Best Paper/Technical Awards at IWWAN06, EMERGING10, BSN 2011, ITST 2011, SENSORNETS 2012, EvoCOMNET 2013, BSN 2014, SoftCOM 2014, and EvoComNet 2015. In 2015, he has been nominated, by the Italian Ministry of Defense, as the only Italian representative (Technical Team Member) in the NATO Panel HFM-260 "Enhancing Warfighter Effectiveness with Wearable Bio Sensors and Physiological Models," in the period 2015-2018. His research interests include wireless networking, signal processing, and Internet of Things. He is senior member of the IEEE.



Matteo Giuberti (GSM'13–M'14) received the BSc and MSc degrees (*summa cum laude*) in telecommunications engineering and the PhD degree in information technologies from the University of Parma, Parma, Italy, in 2008, 2010, and 2014, respectively. He is currently working as a research engineer with Xsens Technologies B.V., Enschede, The Netherlands. He received the first Body Sensor Network (BSN) Contest and ranked second in one task of the Opportunity Challenge in 2011. He also received the Paper Award at BSN 2014. His

research interests include data processing in wireless sensor networks (WSNs) and, more specifically, body sensor networks (BSNs), body area networks (BANs), inertial motion capture and posture recognition, motion reconstruction, activity classification, orientation estimation algorithms, telerehabilitation and mobile health applications, and wireless (indoor) localization. He is a member of the IEEE.



Laura Contin is a senior researcher with the Strategy and Innovation Department, Telecom Italia, Turin, Italy. She has researched and published extensively in multimedia telecommunications, and is currently involved in R&D projects related to active aging, remote rehabilitation, and remote monitoring of neurological patients. She has authored numerous international conference papers, journal papers, and patents. Her research interests include body sensor networks, algorithms for motion tracking, and ambient assisted living.



Veronica Cimolin received the Master's and PhD degrees in bioengineering (with a focus on the quantitative analysis of movement for the assessment of functional limitation in children with Cerebral Palsy), from the Politecnico di Milano, Milan, Italy, in 2002 and 2007, respectively. She is currently a researcher with the Department of Electronics, Information, and Bioengineering, Politecnico di Milano. She is with the "Luigi Divieti" Posture and Movement Analysis Laboratory. She is involved in the activity of several

movement analysis laboratories of national and international institutes. She teaches the course "Impianti ospedalieri e sicurezza" and assists in the teaching of "Laboratorio di valutazione funzionale." She has authored several peer-reviewed international papers. Her research interests include quantitative movement analysis for clinical and rehabilitative applications.



Corrado Azzaro received the degree in medicine and surgery from the University of Palermo, Palermo, Italy, in 2002. He completed his specialty training in clinical neurology with the Neurology Department, "Molinette Hospital," Turin, Italy, in 2011. He has been a visiting doctor with the "Centro de evaluación neurologica para niños y adolescentes" (CENNA), Monterrey, Mexico, from 2002 to 2003, and with the Neurology Department, "Hospital Virgen del Rocío," Sevilla, Spain, in 2003. He is currently working as an assistant

with the Department of Neurology, "San Giuseppe" Hospital, Clinical Research Institute "Istituto Auxologico Italiano," Piacavallo, Verbania, Italy. His research interests include neurophysiology, movement analysis in virtual reality environments, and applied medical informatics.



Giovanni Albani has been a visiting researcher with the Hospital Clinico (1990) and Bellvitge, Barcelona, Spain (1992), and Neurologische Clinic University of Zurich, "Paul Sherrer Institute" Nuclear Medicine Centre Villigen, Switzerland, and "Balgrist" Swiss Paraplegic Zentrum, Zurich, Switzerland (from 1995 to 1997). He received the degree in medicine and surgery from the University of Pavia, Pavia, Italy, in 1992, and completed the School of Neurophysiopathology, Neurological National Institute "Casimiro Mondino," Pavia,

Italy, in 1997. After being Chief of service of neurophysiology in Clinical Hospital "Beato Matteo," Vigevano, Italy (1998-2005). He is currently an assistant with the Department of Neurology, "San Giuseppe" Hospital, Clinical Research Institute "Istituto Auxologico Italiano," Piacavallo-Verbania, Italy. His research interests include movement disorders, movement analysis, neurophysiology, and virtual reality.

Alessandro Mauro is a full professor of neurology with the Department of Neurosciences, Medical School, University of Torino, Turin, Italy, since 2007. Since 2000, he has been the medical director with the University Unit of Neurology and Neurorehabilitation, and with the Laboratory of Neuropathology and Clinical Neurobiology, San Giuseppe Hospital-Istituto Auxologico Italiano-IRCCS, Piacavallo-Oggebbio (VB), Italy. Since 2010, he has been the medical director with the Centre of Sleep Medicine of the same institution. His research interests include clinical neurology, neurogenetics and molecular neuropathology of neurodegenerative diseases, neurorehabilitation, and sleep disorders. He is an active member of National and International Scientific Societies, including, the Italian Association of Neuropathology and Clinical Neurobiology (AINPeNC) of which he was the president from 2011 (current past-president and a Member of the Board of Governors).

▷ For more information on this or any other computing topic, please visit our Digital Library at www.computer.org/publications/dlib.